



# Enhancing efficiency of dye sensitized solar cells based on poly(propylene) carbonate polymer gel electrolytes incorporating double salts

Liaw Poh Yee<sup>1</sup> · N. K. Farhana<sup>1</sup> · Fatin Saiha Omar<sup>1</sup> · V. Sundararajan<sup>1</sup> · Shahid Bashir<sup>1</sup> · Norshahirah M. Saidi<sup>1</sup> · S. Ramesh<sup>1</sup> · K. Ramesh<sup>1</sup>

Received: 13 May 2019 / Revised: 4 July 2019 / Accepted: 26 July 2019 / Published online: 24 August 2019  
© Springer-Verlag GmbH Germany, part of Springer Nature 2019

## Abstract

The performance of dye-sensitized solar cells (DSSCs) depends on the ionic conductivity and flexibility of electrolyte. Gel polymer electrolytes (GPEs) consisting poly(propylene) carbonate (PPC) incorporated with double salts (i.e. calcium iodide (CaI<sub>2</sub>) and tetrabutylammonium iodide (TBAI)) were prepared. X-ray diffraction (XRD) authenticated that the crystallinity of PPC is mitigated after incorporation of different concentrations of CaI<sub>2</sub> and TBAI, which is favourable for ion transportation. Fourier-transform infrared spectroscopy (FTIR) unveils the occurrence of complexation between PPC and the double salts. GPE containing 10% of CaI<sub>2</sub> and 30% of TBAI exhibits the highest ionic conductivity (1.838 mS cm<sup>-1</sup>) with the activation energy of 0.156 eV. The fabricated DSSC employing the optimized GPE exhibits the energy conversion efficiency ( $\eta$ ) of 5.49%, short circuit current density ( $J_{sc}$ ) of 16.6 mA cm<sup>-2</sup>, open circuit voltage ( $V_{oc}$ ) of 0.568 V and fill factor (FF) of 54%.

**Keywords** Dye-sensitized solar cell · PPC · Gel polymer electrolyte · Double salts · Efficiency

## Introduction

Energy is essential to all living organisms on earth where the consumption rate has been increasing from the past decade [1]. The current energy consumption for seven billion people worldwide is about 13 terawatts (TW) and this is expected to go up to about 50 TW in less than 40 years [2]. Instead of using fossil fuels, renewable energy sources are a better option. In 2050, solar energy is expected to be the highest cumulative renewable energy. It is because solar energy is abundant and environmental friendly, thus becomes the best choice for the growing energy demand. Researchers had caught immense attention of dye-sensitized solar cells (DSSCs) from the past few decades since the invention of Gratzel [3]. DSSCs have various advantages such as low material cost and higher energy efficiency compared to the second generation of thin

film solar cell [4]. However, DSSCs face technical challenges in maintaining long-term stability and panel seal problem especially when the employed electrolytes are in liquid form [5]. This is due to the fact that liquid electrolytes are sensitive to temperature and have high volatilisation points where they can expand abruptly over high temperature [6]. There are also some other concerns such as the risk of degradation of platinum counter electrode when using liquid polymer electrolyte. Thus, the replacement of liquid electrolytes with more viscous yet high ionic conductivity electrolytes should be done. Among the replacement electrolytes, gel polymer electrolytes (GPEs) have attracted great attention. GPEs promise better long-term stability, lower material and fabrication costs yet possessing similar advantageous properties of liquid electrolytes [7].

Typically, GPE for DSSC application can be prepared by mixing organic solvents, iodide salts, iodine (as redox mediator) and polymer to create a polymer network matrix. Poly(vinylpyrrolidone) (PVP), polyvinylidene fluoride (PVDF), poly(ethylene oxide) (PEO), poly(vinyl alcohol) (PVA) and poly(propylene) carbonate (PPC) have been widely used as the host polymer in GPE mainly because of their high mechanical strength, flexibility, high chemical stability and environmental friendly [8]. Polypropylene carbonate

✉ S. Ramesh  
rameshtsubra@gmail.com

<sup>1</sup> Centre for Ionics University of Malaya Department of Physics,  
Faculty of Science, University of Malaya, 50603 Kuala  
Lumpur, Malaysia

(PPC) has a carbonate functional group, so it has better interaction with other materials [9]. Furthermore, PPC is colourless and highly amorphous in nature. Several studies had shown improvement in DSSC efficiency when second salts are incorporated in the GPE systems as compared to single salt-based GPE systems [10]. Generally, GPEs which consist of double salts contain two iodide salts with the mixture of different sizes of cations: larger cations (e.g. TEA<sup>+</sup>, TBA<sup>+</sup>, TPA<sup>+</sup>) and smaller cations (e.g. Na<sup>+</sup>, Li<sup>+</sup>, K<sup>+</sup>, Ca<sup>2+</sup>) [11]. The different sizes of cations play different roles in the GPE [12, 13]. Large cation is responsible to separate polymer matrix, creating more space for the movement of smaller cations and iodide ions. In addition, bulky cations with higher mass will have higher anionic energy [14]. Higher energy of iodide anions will increase the efficiency of DSSCs. On the other side, smaller size of cations tends to adsorb more on the surface of titanium dioxide working electrode and increases the rate of electron injection [15]. Most of the reported DSSCs use only single ionic salt system in their GPE with either small cations or large cations, and there are very few that have reported cases of DSSC electrolytes containing two or more different sizes of metal cations. According to some recent studies, there are works reporting that the combination of the two different sizes of metal cations was able to enhance the power conversion efficiency compared to the single metal cation electrolytes. The aim in this strategy is to find the balance of the concentration of the different types of cations added into system. GPE with high number of smaller cations could have very short circuit current density but lower open circuit voltage in their DSSC and vice versa for the GPE with a high concentration of large cations. Thus, having the optimum concentration of these salts could balance out each other advantages and disadvantages which could lead to an increase in the power conversion efficiency of the DSSCs.

In the present work, two systems were prepared. For the first system, GPE was prepared by incorporating PPC with single salt (calcium iodide salt (CaI<sub>2</sub>)) whereas for the second system, GPE was prepared by incorporating PPC with double salts (CaI<sub>2</sub> and tetrabutylammonium iodide (TBAI)). Ca<sup>2+</sup> represents the small cation while TBA<sup>+</sup> represents the large cation. Through electrochemical impedance spectroscopy (EIS) study, GPE with double salts shows almost two-fold enhancement in the ionic conductivity as compared to GPE with single salt [11]. The effect of single and double salts on crystallinity and functional groups of GPE was analysed via X-ray diffraction (XRD) and Fourier-transform infrared spectroscopy (FTIR) techniques. The crystallinity peak of GPE was more broaden after the addition of double salts which supports the trend of ionic conductivity results. For further comparing the practical application of single and double salts in GPEs, DSSCs utilizing all GPEs were assembled and the performance in terms of short circuit voltage, energy conversion efficiency, open circuit voltage and fill factor were presented.

## Experimental section

### Materials

Poly(propylene) carbonate (PPC), calcium iodide salt, tetrabutylammonium iodide salt, ethylene carbonate (EC), propylene carbonate (PC) and ditetrabutylammonium bis(isothiocyanato) bis(2,2'-bipyridyl-4,4'-dicarboxylato) ruthenium(II) dye (N719) were purchased from Sigma-Aldrich. While the redox mediator, iodine (I<sub>2</sub>), was purchased from Friedmann Schmidt Chemical, titanium dioxide (TiO<sub>2</sub>)-P90 and TiO<sub>2</sub>-P25 were obtained from AEROXIDE.

### Preparation of GPE samples

The experiment was divided into two systems: GPE containing single salt (denoted as system 1) and double salt (denoted as system 2). For system 1, firstly, the fixed ratio of EC and PC (1:1) was mixed with CaI<sub>2</sub> salt and iodine and stirred at 110 °C. After the mixture was completely dissolved, certain amount of PPC polymer was added and stirred overnight at lower temperature. It is to ensure that polymer does not degrade through high temperature and to have a homogeneous GPE. Finally, the GPE was allowed to cool to room temperature and ready for characterization and ionic conductivity test. For system 2, the composition of the optimized GPE from system 1 (with the highest ionic conductivity and highest energy efficiency) was selected for the preparation of GPE containing double salts. In this system, the same steps from system 1 were conducted with the addition of TBAI as the second salt. The composition and designation of the prepared GPEs are shown in Table 1.

**Table 1** Compositions of PPC/CaI<sub>2</sub> (single salt system) and compositions of PPC/CaI<sub>2</sub>/TBAI (double salts)-based gel polymer electrolytes

Electrolytes	PPC/CaI <sub>2</sub> contents (%)
P0	100:0
P10	90:10
P20	80:20
P30	70:30
P40	60:40
P50	50:50
Electrolytes	PPC/CaI <sub>2</sub> /TBAI contents (%)
PT10	60:30:10
PT20	60:20:20
PT30	60:10:30
PT40	60:0:40

## Characterizations of GPE samples

The room temperature ionic conductivity and temperature-dependent ionic conductivity studies of the GPEs were tested through EIS using HIOKI 3523-50 LCR Hi-tester (Table 2). The composition, functional groups and shifting of bonds of the GPEs were analysed through Fourier transform infrared spectroscopy (FTIR) using Thermo Scientific Nicolet ISIO smart ITR with the scan range from 4000 to 500  $\text{cm}^{-1}$  wavenumbers (resolution: 1  $\text{cm}^{-1}$ ). The structure of the GPEs was studied via XRD which was carried out using PANalytical Empyrean diffractometer (45 kV), 40 mA) with the  $2\theta$  range from  $5^\circ$  to  $80^\circ$  (step size: 0.0260°).

## Fabrication of DSSC

### Preparation of working electrodes

Firstly, the fluorine-doped tin oxide (FTO) glass was cleaned using ethanol and distilled water to remove dust particle. Two layers of titanium dioxide ( $\text{TiO}_2$ ) were coated on the surface of cleaned FTO glass by using spin coating method (for the first layer) and doctor blade method (for the second layer). The slurry for the first layer of coating was prepared by mixing 0.5 g of commercial P90  $\text{TiO}_2$  (with the particle size of 14 nm) with 2 mL of nitric acid,  $\text{HNO}_3$  (pH = 1), while the slurry for the second layer of coating was prepared by mixing 0.5 g of P25  $\text{TiO}_2$  (with the particle size of 21 nm) with 2 mL of  $\text{HNO}_3$  and a few drops of X-100 triton (to increase the viscosity of P25  $\text{TiO}_2$  slurry). After both slurries were coated on the FTO glass, the FTO glass was sintered at 450 °C for 30 min. The electrodes were allowed to cool to ambient temperature followed by immersing the electrodes into N719 dye for 24 h to ensure that the dye molecules are anchored on the  $\text{TiO}_2$  layer.

### Preparation of counter electrodes

The counter electrode of DSSC was initially prepared by drop casting the mixture of 1 g of chloroplatinic acid solution and 5 mL of ethanol onto the cleaned FTO glass. The coated glass

was then sintered for 30 min at 450 °C and subsequently cleaned using ethanol after the glass is cooled to room temperature. These steps were repeated twice until the desired thickness of platinum coating is achieved.

### Characterization of DSSCs

DSSCs were fabricated with the configuration of glass/FTO/ $\text{TiO}_2$ /dye/GPE/Pt/FTO/glass. The prepared GPEs were sandwiched between working and counter electrodes and connected to Metrohm Autolab potentiostat (PGSTAT128N). The J-V curve of the DSSCs was measured under the simulated sunlight illumination (100  $\text{mW cm}^{-2}$ ) generated by ABET technologies solar simulator.

## Results and discussion

### EIS studies

#### Ionic conductivity at room temperature

The ionic conductivity of GPEs of system 1 (P0–P30) and system 2 (PT0–PT40) was studied via EIS test. The ionic conductivity of GPEs was calculated using the following formula:

$$\sigma = \frac{l}{R_b A}$$

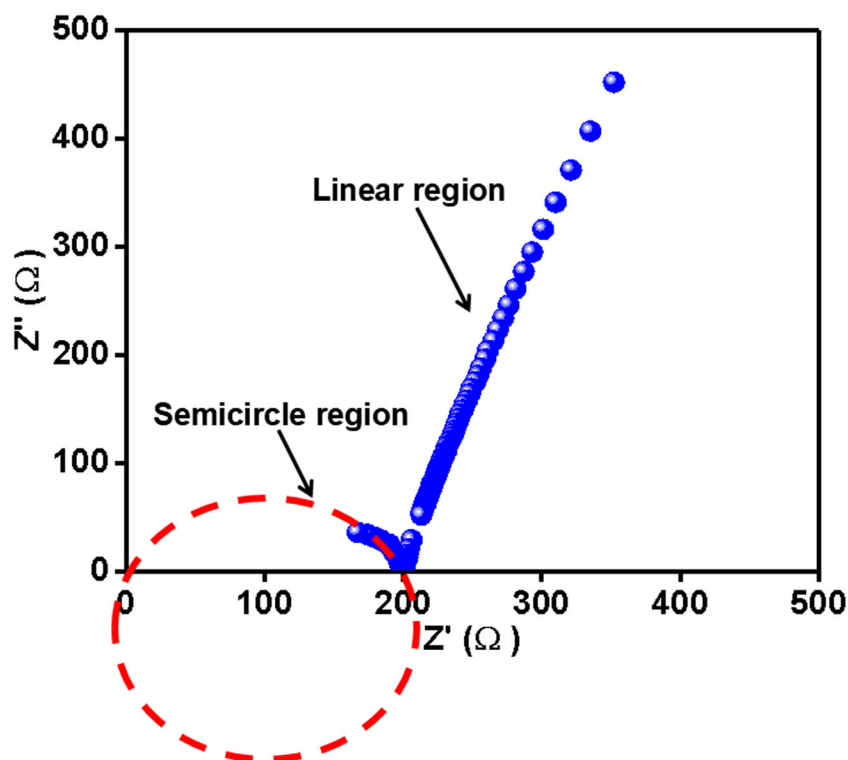
where  $\sigma$ : ionic conductivity ( $\text{S cm}^{-1}$ ),  $l$ : thickness of sample (cm),  $R_b$ : bulk resistance ( $\Omega$ ) and  $A$ : cross-sectional area of the sample ( $\text{cm}^2$ ). The thickness and area of the samples were measured using a micrometre screw gauge while the values of  $R_b$  can be obtained from the intercept of  $x$ -axis in the Cole-Cole plot (displayed in Fig. 1). The  $x$ -axis and  $y$ -axis of the graph were represented by the real complex impedance ( $Z'$ ) and imaginary impedance ( $Z''$ ), respectively. The Cole-Cole plot can be split into two regions: linear region at the low frequency and semicircle region at the high frequency. The linear region can be assigned to the ionic conduction of GPEs and semicircle region is contributed from the blocking electrodes [16].

As shown in Fig. 2a, GPE sample prepared using pure PPC exhibits the lowest ionic conductivity of 0.001  $\text{mS cm}^{-1}$ . It is undoubtedly because the pure PPC polymer molecules are bonded tightly together and thus no ions were free to conduct. With the addition of  $\text{CaI}_2$  salt, an abrupt increase in ionic conductivity was observed with the highest ionic conductivity value of 0.455  $\text{mS cm}^{-1}$  after the addition of 10 wt.%  $\text{CaI}_2$  salt. The GPE sample in the system 1 has only the  $\text{CaI}_2$  salt with smaller cation  $\text{Ca}^{2+}$  which can be mobile, and therefore, its ionic conductivity must come from the contributions of

**Table 2** The comparison for the efficiency of some DSSCs

	Electrolytes system (polymer-salt)	$\eta$ (%)	References
Single salt	P(VB-co-VA-co-Vac)-TPAI	4.61	[26]
	PAN-TBAI	4.16	[27]
	PAN-MgI <sub>2</sub>	2.0	[18]
Double salt	PAN-MgI <sub>2</sub> -Hex <sub>4</sub> N <sup>+</sup> I <sup>-</sup>	3.1	[18]
	P(VP-co-Vac)-NaI-TBAI	4.54	[28]
	PVdF-KI-Pr <sub>4</sub> N <sup>+</sup> I <sup>-</sup>	5.36	[29]

**Fig. 1** Cole-Cole impedance plot of P20 at room temperature with two different regions



both  $\text{Ca}^{2+}$  and  $\Gamma$  ions. The change in ionic conductivity values upon the addition of  $\text{CaI}_2$  salt can be exemplified by the following equation:

$$\sigma = nq\mu$$

where  $n$ : ion concentration,  $q$ : charge of mobile ion,  $\mu$ : ion mobility and  $\sigma$ : ionic conductivity ( $\text{S cm}^{-1}$ ). Based on this equation, the higher ionic conductivity of the GPE after the addition of  $\text{CaI}_2$  salt is contributed from the increase in ion concentration and their mobility [17]. The increase in ion mobility is related to the crystallinity of GPE. In general, the lower the crystallinity of GPE, the higher the ion mobility within the polymer matrix. This concept explains the elevation of ionic conductivity from 0 to 40% of  $\text{CaI}_2$ . However, at higher  $\text{CaI}_2$  salt concentration, the ionic conductivity was slightly decreased because the higher crystallinity of the GPE reduced the ion mobility. Figure 2b compares the ionic conductivity of all GPEs in system 2. After the addition of TBAI salt to P40 (chosen due to its highest ionic conductivity from system 1), the ionic conductivity was further increased. The highest ionic conductivity in system 2 is shown by PT30, in which the ionic conductivity increases almost two folded, from  $0.595 \text{ mS cm}^{-1}$  (for P40) to  $1.838 \text{ mS cm}^{-1}$  after the addition of TBAI salt (i.e. 10 wt.% of  $\text{CaI}_2$  salt and 30 wt.% of TBAI salt). At the given salt concentration combination, the dissociated  $\text{Ca}^{2+}$  and  $\Gamma$  ions from  $\text{CaI}_2$  salt and  $\Gamma$  ions from TBAI salt will take part in the conduction process and contribute

to the ionic conductivity of the GPEs [18]. The conductivity (or the number of ionic charge carrier) increases with the increase in the amount of  $\text{TBA}^+\Gamma^-$ . This is contributed from the lower lattice energy of  $\text{TBA}^+\Gamma^-$  ( $320.8 \text{ kJ mol}^{-1}$ ) than that of  $\text{CaI}_2$  ( $1735.1 \text{ kJ mol}^{-1}$ ) which led to the higher degree of  $\text{TBA}^+\Gamma^-$  salt dissociation [19]. Generally, when a salt has lower lattice energy, the dissociation of ion will be higher and thus the ions have more freedom to interact with the functional groups of PPC [20]. In addition, the presence of bulky cation ( $\text{TBA}^+$ ) can impose more disorder on long polymer chains and it can make long polymer chains more separated [21]. Thus, it allows small cation ( $\text{Ca}^{2+}$ ) to move around the polymer matrix easily and subsequently results in a significant enhancement in ionic conductivity as compared to single salt system. The total conductivity originates from mobile  $\text{Ca}^{2+}$  cations, and  $\Gamma^-$  anions from both salts and therefore the total conductivity naturally increase with increasing TBAI content as seen from Fig. 2b.

### Temperature-dependent studies

Figure 2c and d plots a variation of  $\log \sigma$  versus temperature for all GPEs from system 1 and system 2, as a result of based on temperature-dependent studies conducted at temperatures ranging from 303 to 353 K. Deriving from all linear curves in the graphs with the average regression lines near to 1, it indicates that the conductivity of all GPEs obeys Arrhenius theory with the equation as shown below.

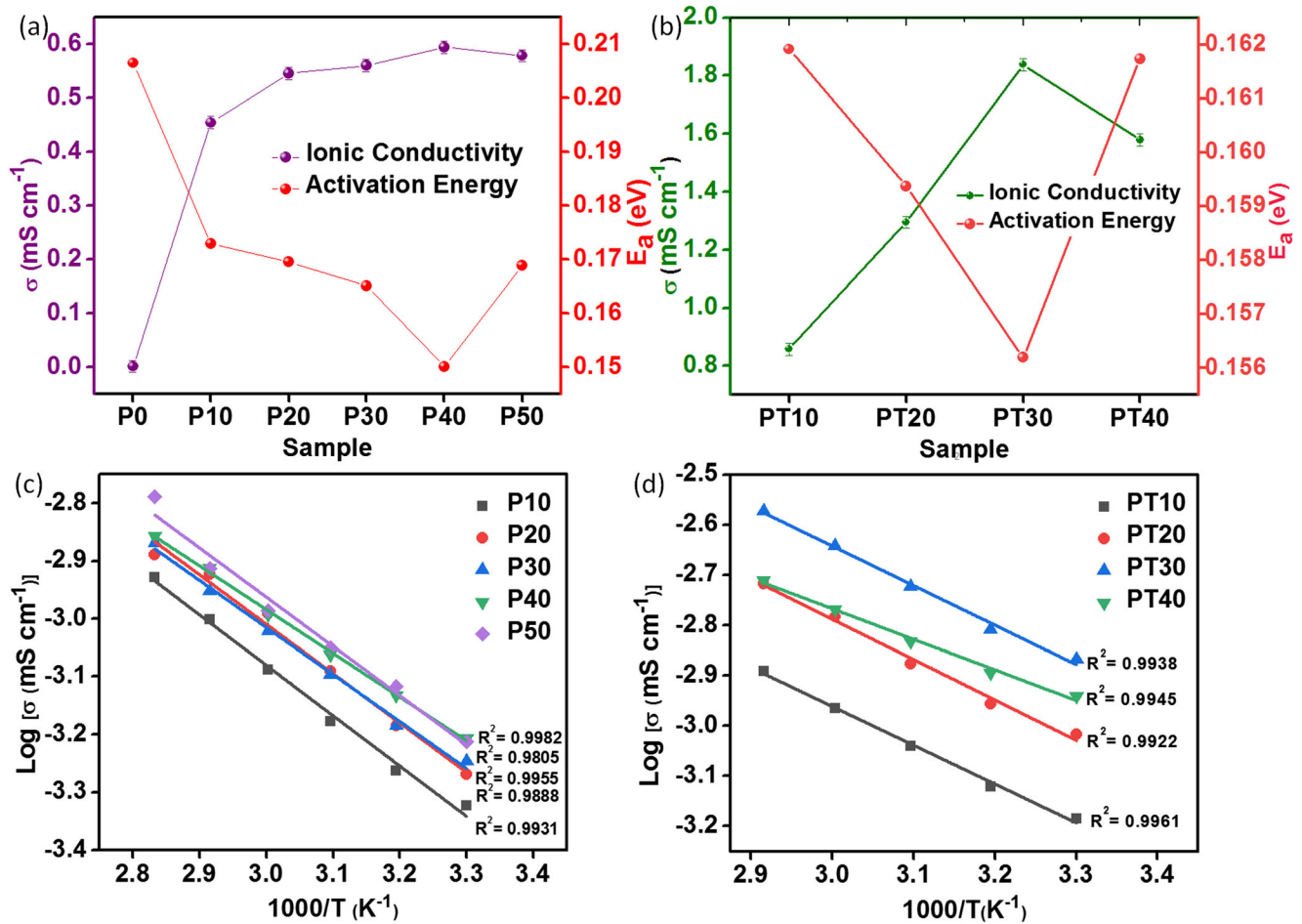


**Fig. 2** Graph of ionic conductivity and activation energy of **a** system 1 and **b** system 2 GPEs with different percentage of salts at room temperature. Graph of logarithmic ionic conductivities at room temperature and against 1000/T for **c** system 1 and **d** system 2 GPEs which follow Arrhenius theory

$$\sigma = \sigma_0 e^{\left(\frac{-E_a}{kT}\right)}$$

where  $\sigma$ : ionic conductivity  $S\ cm^{-1}$ ,  $\sigma_0$ : pre-exponential constant ( $S\ cm^{-1}$ ),  $T$ : temperature (K),  $k$ : Boltzman constant ( $eV\ K^{-1}$ ) and  $E_a$ : activation energy (eV). Linear curves also signify that no phase transition was occurring during the experiment, which is expected for amorphous GPE. Based on the results, the higher the temperature, the higher the ionic conductivity of GPEs. It is because when polymer chains are at the elevated temperature, the thermal energy causes the polymer to vibrate, and thus, eased the rotation of bond and enhanced the interchain and intrachain segmental motion. When the movements of cations increase, the opportunity of ion hopping was greatly increasing and ultimately lower the activation energy of ions. Activation energy is the minimum energy required for the ions to conduct [22]. The trend of activation energy is generally true because ion requires less energy to conduct and thus the ionic conductivity increases. Besides that, by increasing the temperature, the number of disorders and conduction path also increases [23].

### Complexation studies

#### FTIR analysis

FTIR is an important technique to discover the functional group and interaction among the materials. The results of Fourier transform infrared (FTIR) spectroscopy of system 1 and system 2 are displayed in Fig. 3a and b, respectively. Several peaks can be observed at the wavelength range of 1350–1480, 1670–1820 and 1000–1300 in system 1 and system 2, representing the bending of C–H bond, stretching of C=O bond and stretching of C–O–C bond, respectively [24]. Complexation of  $Ca_2$  salt, TBAI salt and PPC was suspected. The bending of C–H bond was shifted to a lower wavenumber from 1396 to 1392  $cm^{-1}$ , 1391  $cm^{-1}$  and 1391  $cm^{-1}$  for the GPEs studied, while the stretching of C–O–C bond also shifted from 1170  $cm^{-1}$  to a lower wavenumber (1161  $cm^{-1}$ , 1160  $cm^{-1}$  and 1159  $cm^{-1}$ ). In addition, the intensity of bending of C–H bond and stretching of C–O–C bond was increased comparing the P0 and other GPEs studied as shown



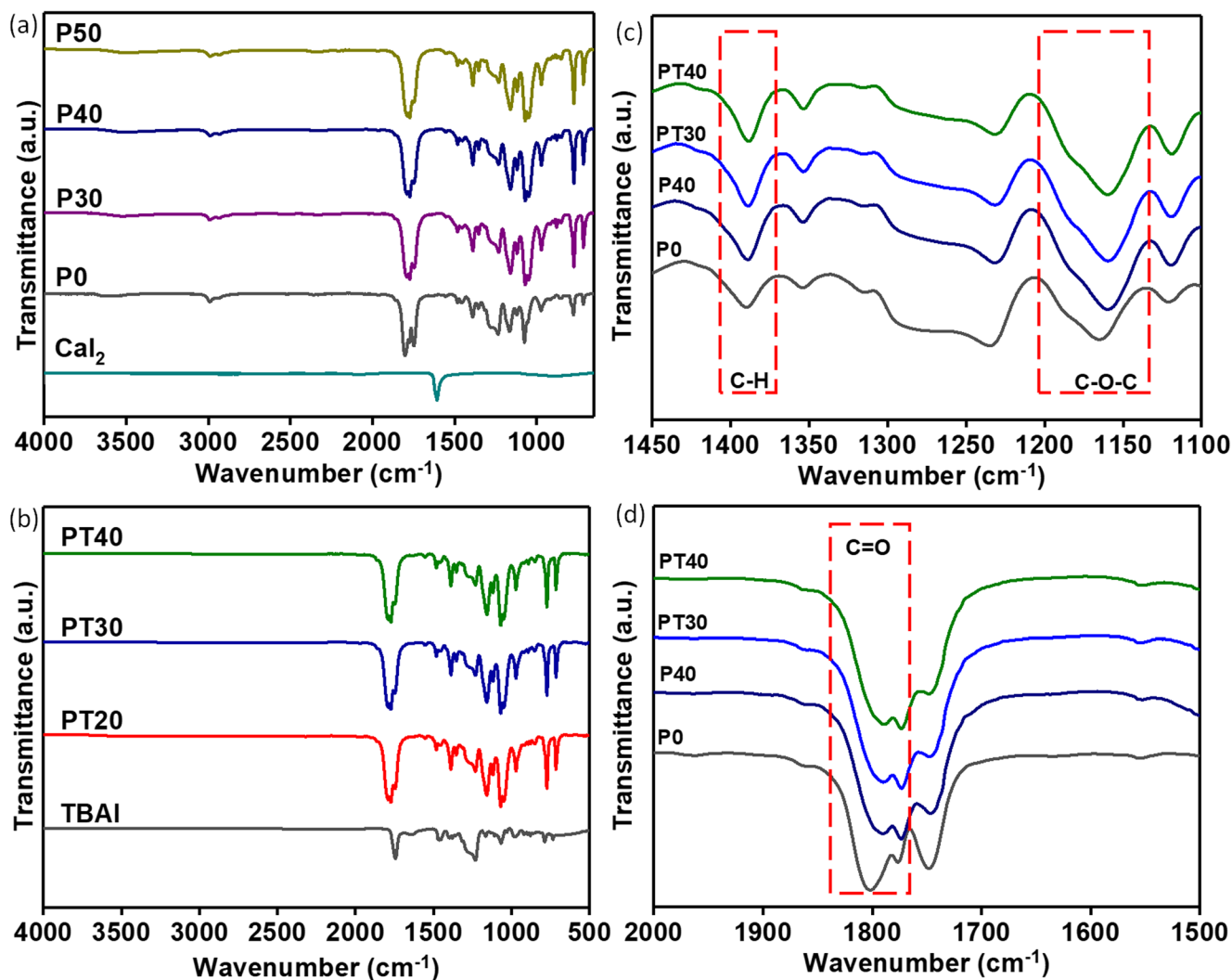


Fig. 3 FTIR spectra of **a** system 1 (pure  $\text{CaI}_2$  salt, P0, P30, P40 and P50), **b** system 2 (pure TBAI salt, PT20, PT30 and PT40)

in Fig. 3c. Based on the FTIR spectra studied, it shows that the interaction had occurred.

From Fig. 3d, the band at  $1801\text{ cm}^{-1}$  is referring to the stretching vibration of the C=O bond in pure PPC [9, 25]. The band can be seen become broad as the  $\text{CaI}_2$  and TBAI

into the system. This is due to the fact that new band exists at the lower range of wavenumbers and there are two bands blend together to form a broad band. This is shown that there is interaction between the  $\text{Ca}^{2+}$  ion and  $\text{TBA}^+$  with the carbonyl oxygen group of PPC. Moreover, the bending of C=O

Fig. 4 XRD spectra for the range of  $0^\circ$  to  $80^\circ$  of **a** system 1 (pure  $\text{CaI}_2$  salt, P0, P30, P40 and P50) and **b** system 2 (pure TBAI salt, PT20, PT30 and PT40)

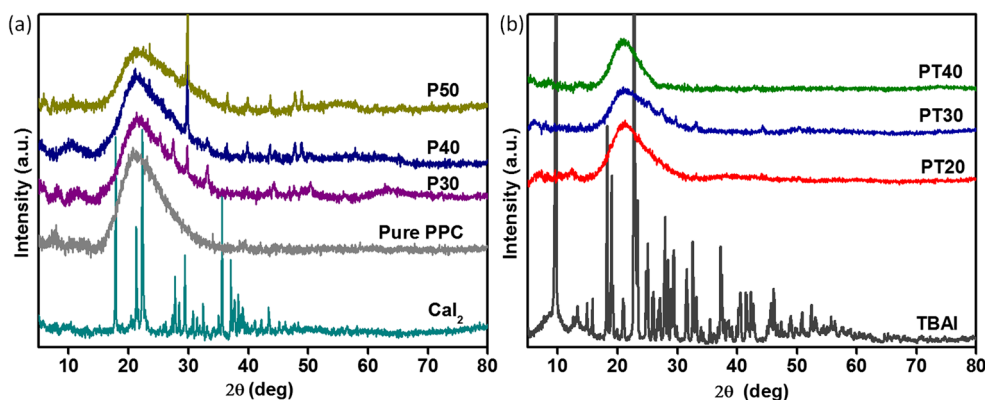
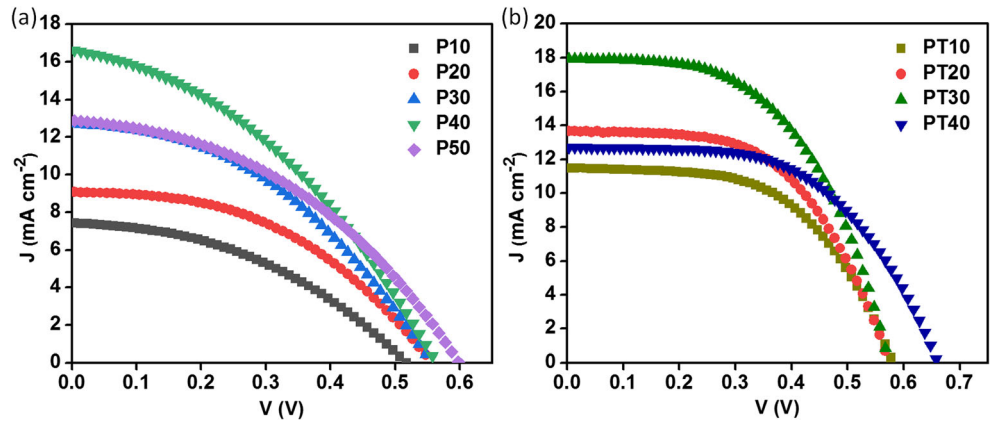


**Fig. 5** Plot of current density,  $J$  against potential,  $V$  of DSSCs for all GPEs prepared in **a** system 1 and **b** system 2



bond was shifted to a higher wavenumber from  $1801$  to  $1776\text{ cm}^{-1}$  and  $1773\text{ cm}^{-1}$  for the GPEs studied. Besides that, from the figure, it shows that the intensity at band  $1801\text{ cm}^{-1}$  decreases in the intensity. This is proven that there is complexation between the PPC and  $\text{CaI}_2$  and TBAI salts. The interaction among them causes the backbone of PPC slightly shifted to a higher wavenumber nearby peaks.

**XRD analysis**

XRD test was carried out to determine the structural of samples. Figure 4a and b shows the XRD diffractogram of pure PPC, pure  $\text{CaI}_2$ , pure TBAI, all GPEs from system 1 and system 2, respectively. In Fig. 4a,  $\text{CaI}_2$  salt has a series of sharp peaks which indicates that it has crystalline

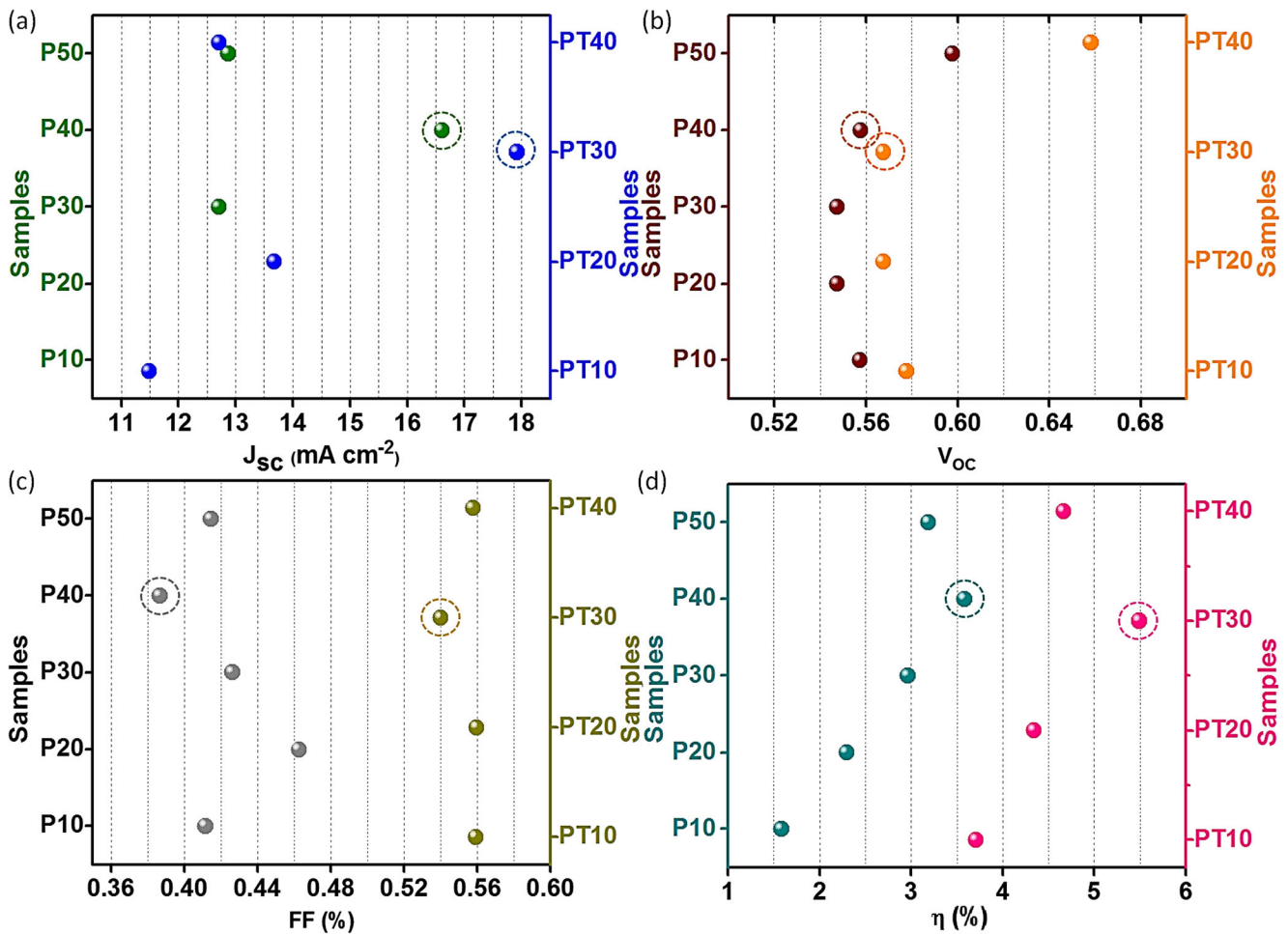


**Fig. 6** Graphs of **a** short circuit current density,  $J_{sc}$ , **b** open circuit voltage  $V_{oc}$ , **c** fill factor and **d** energy conversion efficiency,  $\eta$  of DSSCs tested using GPEs prepared in system 1 and system 2

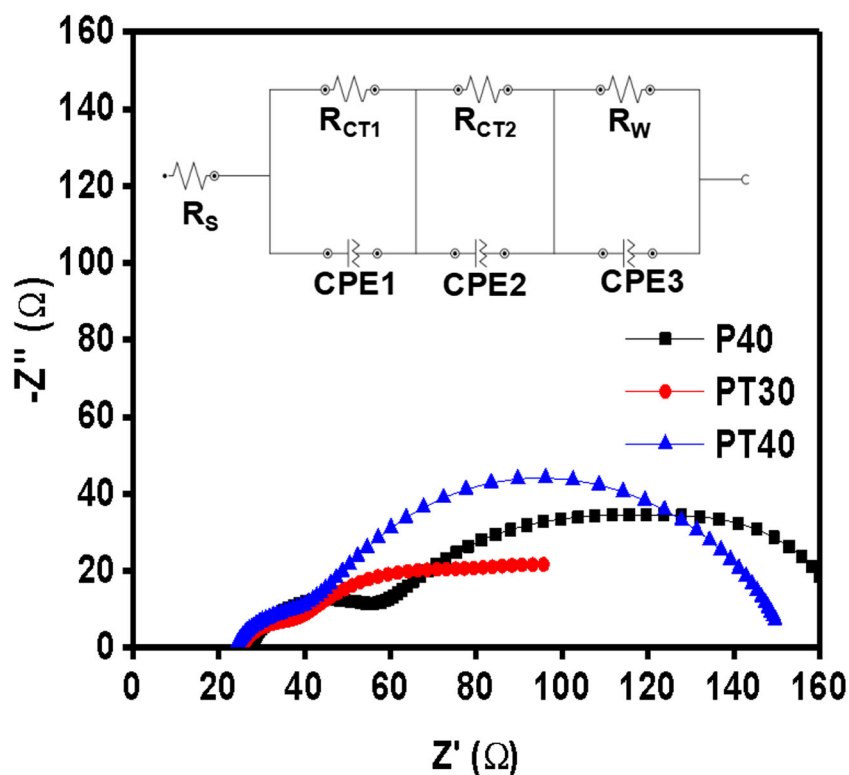
structure. A single broad peak was present in all GPEs which shows that the GPEs were amorphous. However, there was emergence of a significant sharp peak at  $29.38^\circ$  which shows that the crystallinity of P50 was higher compared to P30 and P40. An emerging and shifting of sharp peaks (which occurred at  $35.33^\circ$ ,  $40.29^\circ$  and  $43.27^\circ$ ) have proven that the interaction between calcium iodide salts and polypropylene carbonate polymer has taken place. Besides, the occurrence of the sharp peak with highest intensity in P50 indicates significant presence of semi crystalline structures which can be linked to undissolved calcium iodide salt. XRD analysis for system 2 is shown in Fig. 4b where no sharp peaks were observed. This observation explains for the higher ionic conductivity and higher energy efficiency obtained for system 2 as compared to system 1. Highly amorphous polymer electrolyte systems improve ion mobility which in turn promotes better ionic conductivity [26]. Besides, broader peaks were seen for PT30 compared to PT20 and PT40 which signifies the reduction in crystalline nature of the GPEs.

### Photovoltaic performance

Figure 5a and b portrays the J-V characteristics of the fabricated DSSCs employing all GPEs from system 1 and system 2, while Fig. 6 shows the value of DSSC parameters: short-

circuit current density ( $J_{sc}$ ), open circuit voltage ( $V_{oc}$ ), fill factor (FF) and energy efficiency ( $\eta$ ), which were obtained from the J-V characteristics curves. Based on the figures, the maximum  $J_{sc}$  achieved for system 1 and system 2 were  $16.6 \text{ mA cm}^{-2}$  and  $17.9 \text{ mA cm}^{-2}$ , respectively, whereas the maximum  $\eta$  obtained for system 1 and system 2 were 3.58% and 5.49%, respectively. The augmentation in  $J_{sc}$  and  $\eta$  observed from system 1 to system 2 proof GPE containing double salts is better GPE containing single salt [14].  $V_{oc}$  is somewhat large for larger cation  $\text{TBA}^+$ , but for the smaller cation  $\text{Ca}^{2+}$ ,  $V_{oc}$  is small. On mixing the two cations,  $V_{oc}$  drops a little and increases again as the amount of  $\text{TBA}^+$  increases. The double salt system shows an increment in  $V_{oc}$  of 0.58 V for the highest sample (PT30) compared to single salt system due to the effect of both types of cations. The fill factor for double salt system also shows an increment from 39 to 54% due to the fact that charge accumulation is lessening as the shape of the J-V curves becomes more rectangular form compared to single salt system. In the double salt system (system 2), the  $J_{sc}$  reaches a maximum value for a combination of the mixed cations as shown in Fig. 6. As the percentage of TBAI increases, the net iodide ion concentration ( $\Gamma^-$ ) in the GPE also increases and contributes to increase in  $J_{sc}$ . This is due to the reason of the bulky cations (TBAI) that have higher degree of salt dissociation due to their lower lattice energy ( $320.8 \text{ kJ mol}^{-1}$ ) as compared to  $\text{CaI}_2$  ( $1735.1 \text{ kJ mol}^{-1}$ ). TBAI plays a role in supplying sufficient amount of iodide

Fig. 7 EIS of DSSC





ions in the system and separates the polymer matrix for swifter movement of small cations. On the other hand, the interaction between small cations and  $\text{TiO}_2$  causes positive shift of the flat band potential of the semiconductor and formation of electron trapping states that have increased the rate of electron injection and eventually increases the  $J_{sc}$  [26]. Thus, this proves that double cation system can improve ionic conductivity as well as the efficiency. Table 2 shows the comparison for the efficiency of some DSSCs in other published work based on single salt system and double salt system. Based on this work, it has been shown that significant improvement has been achieved in improving of the GPEs based on double salt system. The DSSC properties are also equivalent or even better compared to the other single or double salts system.

To further investigate the impedance present in the assembled DSSC, EIS data was collected for both systems. The data obtained together with fitted equivalent circuit is shown in Fig. 7 and the corresponding parameters are tabulated in Table 3. Two semicircles can be seen; the first semicircle at high frequency region corresponds to charge transfer resistance at the platinum counter electrode and electrolyte interface ( $R_{CT1}$ ), whereas the second semicircle at lower frequency region denotes the charge transfer resistance of recombination between the  $\text{TiO}_2$  layer and triiodide ions ( $R_{CT2}$ ). It is also clear that the plots do not start from zero indicating the presence of series resistance ( $R_s$ ) due to FTO substrate. Since the values of  $R_s$  do not vary much, thus the influence of  $R_s$  on the efficiency of the DSSCs can be assumed negligible. As shown in Table 3, the value of  $R_{CT2}$  was seen to be the highest for PT40 and lowest for PT30. As  $V_{oc}$  values were previously reported to be in relation with rate of charge recombination process in electrolytes, increase in  $R_{CT2}$  would produce higher  $V_{oc}$  values [27, 30]. This agrees with the J-V data obtained whereby  $V_{oc}$  values recorded for PT40 is the highest at 0.658 V. Despite having a large contact resistance at Pt counter electrode/electrolyte interface, PT30 has the lowest Warburg resistance ( $R_w$ ), which is contributed by the ion diffusion in the GPE. The saturation of ions in PT40 causes a higher diffusion resistance whereas for P40, it can be owed to the stronger ionic interaction of the  $\text{Ca}^{2+}$  ions with polymer backbone that dampens smooth diffusion. A combination of low ion diffusion resistance and reasonably high recombination resistance has contributed to the higher efficiency of the DSSCs.

**Table 3** Parameter of DSSC EIS

Electrolytes.	$R_s$ ( $\Omega$ )	$R_{CT1}$ ( $\Omega$ )	$R_{CT2}$ ( $\Omega$ )	$R_w$ ( $\Omega$ )
P40	27.4	26.2	83.1	29.9
PT30	25.5	34.8	59.1	13.5
PT40	23.8	17.9	91.2	19.8

## Conclusion

GPEs containing polypropylene carbonate host polymer incorporated with various amounts of single salt and double salt were prepared and studied. DSSC performances have shown improvement in double salt system due to the high charge density of ion presence in the electrolyte compared to a single salt system. Double salt system has increased the ionic conductivity from  $0.595 \text{ mS cm}^{-1}$  (for single salt system) to  $1.838 \text{ mS cm}^{-1}$ . Arrhenius theory was obeyed by both systems in which the ion mobility increases with the increment of temperature. FTIR studies had shown complex formation between polymer and double salts through the shifting of bonds. Crystallinity of GPEs was reduced when the salt concentration increases based on the XRD results. The best photovoltaic performance of DSSC among both systems was obtained by PT30 with  $J_{sc}$  of  $17.9 \text{ mA cm}^{-2}$ ,  $\eta$  of 5.49%,  $V_{oc}$  0.57 V and FF of 54%.

**Funding information** This work is financially supported by Fundamental Research Grant Scheme (FRGS) from Ministry of Education, Malaysia (FP062-2018A).

## References

- Ganesan S, Mathew V, Rathika R, Muthuraaman B, Maruthamuthu P, Suthanthiraraj SA, Kim J (2018) Low-cost tetra ethylene glycol derivatives in polymer blend electrolytes for dye-sensitized solar cells with high photovoltaic conversion efficiencies. *Mater Sci Eng B Solid-State Mater Adv Technol* 229:37–43. <https://doi.org/10.1016/j.mseb.2017.12.016>
- Latip NAA, Ng HM, Farah N, Ramesh K, Ramesh S, Ramesh S (2017) Novel development towards preparation of highly efficient ionic liquid based co-polymer electrolytes and its application in dye-sensitized solar cells. *Org Electron Phys Mater Appl* 41:33–41. <https://doi.org/10.1016/j.orgel.2016.11.040>
- Grätzel M (2003) Dye-sensitized solar cells. *J Photochem Photobiol C Photochem Rev* 4:145–153. [https://doi.org/10.1016/S1389-5567\(03\)00026-1](https://doi.org/10.1016/S1389-5567(03)00026-1)
- Bandara TMWJ, Weerasinghe AMJS, Dissanayake MAKLL, Senadeera GKR, Furlani M, Albinsson I, Mellander BE (2018) Characterization of poly (vinylidene fluoride-co-hexafluoropropylene) (PVdF-HFP) nanofiber membrane based quasi solid electrolytes and their application in a dye sensitized solar cell. *Electrochim Acta* 266:276–283. <https://doi.org/10.1016/j.electacta.2018.02.025>
- Buraidah MH, Shah S, Teo LP, Chowdhury FI, Careem MA, Albinsson I, Mellander BE, Arof AK (2017) High efficient dye sensitized solar cells using phthaloylchitosan based gel polymer electrolytes. *Electrochim Acta* 245:846–853. <https://doi.org/10.1016/j.electacta.2017.06.011>
- Jayaweera EN, Ranasinghe CSK, Kumara GRA, Wanninayake WMNMB, Senarathne KGC, Tennakone K, Rajapakse RMG, Ileperuma OA (2015) Novel method to improve performance of dye-sensitized solar cells based on quasi-solid gel-polymer electrolytes. *Electrochim Acta* 152:360–367. <https://doi.org/10.1016/j.electacta.2014.11.156>
- Senthil RA, Theerthagiri J, Madhavan J, Ganesan S, Arof AK (2017) Influence of organic additive to PVDF-HFP mixed iodide

- electrolytes on the photovoltaic performance of dye-sensitized solar cells. *J Phys Chem Solids* 101:18–24. <https://doi.org/10.1016/j.jpics.2016.10.007>
8. Tan CY, Farhana NK, Saidi NM, Ramesh S, Ramesh K (2018) Conductivity, dielectric studies and structural properties of P(VA-co-PE) and its application in dye sensitized solar cell. *Org Electron Phys Mater Appl* 56:116–124. <https://doi.org/10.1016/j.orgel.2018.02.007>
  9. Zhou D, Zhou R, Chen C, Yee WA, Kong J, Ding G, Lu X (2013) Non-volatile polymer electrolyte based on poly(propylene carbonate), ionic liquid, and lithium perchlorate for electrochromic devices. *J Phys Chem B* 117:7783–7789. <https://doi.org/10.1021/jp4021678>
  10. Yusuf SNF, Azzahari AD, Yahya R, Majid SR, Careem MA, Arof AK (2016) From crab shell to solar cell: a gel polymer electrolyte based on N-phthaloylchitosan and its application in dye-sensitized solar cells. *RSC Adv* 6:27714–27724. <https://doi.org/10.1039/c6ra04188d>
  11. Khan MZH, Al-Mamun MR, Halder PK, Aziz MA (2017) Performance improvement of modified dye-sensitized solar cells. *Renew Sust Energ Rev* 71:602–617
  12. Wanninayake WMNMB, Premaratne K, Kumara GRA, Rajapakse RMG (2016) Use of lithium iodide and tetrapropylammonium iodide in gel electrolytes for improved performance of quasi-solid-state dye-sensitized solar cells: recording an efficiency of 6.40%. *Electrochim Acta* 191:1037–1043. <https://doi.org/10.1016/j.electacta.2016.01.108>
  13. Watson DF, Meyer GJ (2004) Cation effects in nanocrystalline solar cells. *Coord Chem Rev* 248:1391–1406
  14. Madhushani W, Jayathilake Y, Perera K, Vidanapathirana K (2016) Effect of cation size of iodide salt in the electrolyte on the performance of dye sensitized solar cells. *J Natl Sci Found Sri Lanka* 44:77. <https://doi.org/10.4038/jnsfsr.v44i1.7984>
  15. Kumar D, Hashmi SA (2010) Ion transport and ion-filler-polymer interaction in poly(methyl methacrylate)-based, sodium ion conducting, gel polymer electrolytes dispersed with silica nanoparticles. *J Power Sources* 195:5101–5108. <https://doi.org/10.1016/j.jpowsour.2010.02.026>
  16. Zebardastan N, Khanmirzaei MH, Ramesh S, Ramesh K (2017) Performance enhancement of poly (vinylidene fluoride-co-hexafluoro propylene)/polyethylene oxide based nanocomposite polymer electrolyte with ZnO nanofiller for dye-sensitized solar cell. *Org Electron Phys Mater Appl* 49:292–299. <https://doi.org/10.1016/j.orgel.2017.06.062>
  17. Aziz SB, Woo TJ, Kadir MFZ, Ahmed HM (2018) A conceptual review on polymer electrolytes and ion transport models. *J Sci Adv Mater Devices* 3:1–17. <https://doi.org/10.1016/j.jsamd.2018.01.002>
  18. Bandara TMWJ, Dissanayake MAKL, Jayasundara WJMJSR, Albinsson I, Mellander BE (2012) Efficiency enhancement in dye sensitized solar cells using gel polymer electrolytes based on a tetrahexylammonium iodide and MgI<sub>2</sub> binary iodide system. *Phys Chem Chem Phys* 14:8620–8627. <https://doi.org/10.1039/c2cp24139k>
  19. Dissanayake MAKL, Thotawatthage CA, Senadera GKR, Bandara TMWJ et al (2012) Efficiency enhancement by mixed cation effect in dye-sensitized solar cells with PAN based gel polymer electrolyte. *J Photochem Photobio A: Chem* 246:29–35
  20. Ng HM, Ramesh S, Ramesh K (2015) Efficiency improvement by incorporating 1-methyl-3-propylimidazolium iodide ionic liquid in gel polymer electrolytes for dye-sensitized solar cells. *Electrochim Acta* 175:169–175. <https://doi.org/10.1016/j.electacta.2015.01.076>
  21. Ming NH, Ramesh S, Ramesh K (2016) The potential of incorporation of binary salts and ionic liquid in P(VP-co-VAc) gel polymer electrolyte in electrochemical and photovoltaic performances. *Sci Rep* 6:1–13. <https://doi.org/10.1038/srep27630>
  22. Sundararajan V, Selvaraj G, Ng HM, Ramesh S, Ramesh K, Wilfred CD, Bashir S (2017) Exploring the effect of novel N-butyl-6-methylquinolinium bis(trifluoromethylsulfonyl)imide ionic liquid addition to poly(methyl methacrylate-co-methacrylic) acid electrolyte system as employed in gel-state dye sensitized solar cells. *Electrochim Acta* 240:361–370. <https://doi.org/10.1016/j.electacta.2017.04.097>
  23. Bandara TMWJ, Dissanayake MAKL, Albinsson I, Mellander BE (2010) Dye-sensitized, nano-porous TiO<sub>2</sub> solar cell with poly(acrylonitrile): MgI<sub>2</sub> plasticized electrolyte. *J Power Sources* 195:3730–3734. <https://doi.org/10.1016/j.jpowsour.2009.11.148>
  24. Farhana NK, Khanmirzaei MH, Ramesh S, Ramesh K (2017) Exploration on polypropylene carbonate polymer for gel polymer electrolyte preparation and dye-sensitized solar cell application. *J Appl Polym Sci* 134:1–6. <https://doi.org/10.1002/app.45091>
  25. Farhana NK, Khanmirzaei MH, Omar FS, Ramesh S, Ramesh K (2017) Ionic conductivity improvement in poly (propylene) carbonate-based gel polymer electrolytes using 1-butyl-3-methylimidazolium iodide (BmimI) ionic liquid for dye-sensitized solar cell application. *Ionics (Kiel)* 23:1601–1605. <https://doi.org/10.1007/s11581-017-1979-z>
  26. Farhana NK, Ramesh S, Ramesh K (2019) Efficiency enhancement of dye-sensitized solar cell based gel polymer electrolytes using poly(vinyl butyral-co-vinyl alcohol-co-vinyl acetate)/tetrapropylammonium iodide. *Mater Sci Semicond Process* 91:414–421. <https://doi.org/10.1016/j.mssp.2018.12.007>
  27. Bandara TMWJ, Jayasundara WJMJSR, Dissanayake MAKL, Furlani M, Albinsson I, Mellander BE (2013) Effect of cation size on the performance of dye sensitized nanocrystalline TiO<sub>2</sub> solar cells based in quasi-solid state PAN electrolytes containing quaternary ammonium iodides. *Electrochim Acta* 109:609–616
  28. Robin S, Ming NH, Ramesh S, Ramesh K (2016) Amelioration of electrochemical and photovoltaic performances on P(VP-co-Vac) based gel polymer electrolytes by incorporating double salts for dye-sensitized solar cells. *J Appl Polym Sci* 43805. <https://doi.org/10.1002/app.43805>
  29. Arof AK, Aziz MF, Noor MM, Careem MA, Bandara LRAK, Thotawatthage CA, Rupasinghe WNS, Dissanayake MAKL (2014) Efficiency enhancement by mixed cation effect in dye-sensitized solar cells with a PVdF based gel polymer electrolyte. *Int J Hydrog Energy* 39:2929–2935
  30. Sharma GD, Daphnomili D, Angaridis PA, Biswas S, Coutsolelos AG (2013) Effect of thiourea incorporation in the electrolyte on the photovoltaic performance of the DSSC sensitized with pyridyl functionalized porphyrin. *Electrochim Acta* 102:459–465. <https://doi.org/10.1016/j.electacta.2013.04.003>

**Publisher's note** Springer Nature remains neutral with regard to jurisdictional claims in published maps and institutional affiliations.